High-Yield Synthesis of Multi-Branched Urchin-Like Gold Nanoparticles

Osman M. Bakr,[†,‡] Benjamin H. Wunsch,[†] and Francesco Stellacci*[,†]

Department of Materials Science and Engineering, Massachusetts Institute of Technology, 77 Massachusetts Avenue, Cambridge, Massachusetts 02139, and Division of Engineering and Applied Sciences, Harvard University, 29 Oxford Street, Cambridge, Massachusetts 02138

Received March 21, 2006. Revised Manuscript Received May 10, 2006

Here, we report on an aqueous room temperature synthesis method for the production of gold nanoparticles that have a number (>4) of branches ultimately resembling the shape of sea urchins. The particles are synthesized in the presence of water soluble thiol terminated molecules, used as ligand molecules. These nano-urchins are produced in high yield and exhibit unique optical properties. The thiolated ligands stabilize the particles, making it possible to dry them and store them for days. When redissolved, the particles show some aggregation but not a loss in shape; their extinction spectrum shows a shift in the plasmon resonance from 585 to 622 nm together with a peak broadening. Large local electromagnetic (EM) field enhancements are expected near the sharp featured branches of the nano-urchins. Finite difference time-domain (FDTD) calculations performed on a nanoparticle with four branches show enhancements of the light intensity relative to the incident field of approximately 3000-fold. We reason that these particles will find applications as materials for surface enhanced Raman scattering (SERS).

Introduction

Research on nanoparticles is driven by their many potential applications ranging from photonics[1−4] to biology[5−8] and catalysis.[9] At present, there is considerable interest in producing odd-shaped particles to exploit their unique optical and electronic properties.[10−13] Metal nanoparticles have been produced in many different shapes and sizes,[12,14−17] from prisms[18,19] to tetrapods.[20−24] Here, we report on a simple room temperature method for the synthesis and purification of multi-branched gold nanoparticles whose shape resembles that of sea urchins. Hence, hereafter we refer to these nanoparticles as nano-urchins.

Multi-branched metallic nanoparticles have been synthesized before. Chen et al.[16] reported on the silver plate seeded synthesis of gold monopods, bipods, tripods, and tetrapods using the surfactant cetyltrimethylammonium bromide (CTAB) as a capping agent. Their synthesis resulted in a mixture of all four types of nanoparticles with tripods and tetrapods representing only a small fraction (∼12%). Hao et al.[25] also reported on the synthesis of gold tripods using bis-(*p*-sulfonatophynyl)phenylphosphine dihyrate dipotassium as a stabilizer. Multi-pods of metallic particles were first presented by Sau et al.;[17] seeds of gold nanoparticles were grown by reducing gold salts in the presence of CTAB. Nanoparticles with a variety of shapes and morphologies were obtained in high yields, including multi-branched (> branches) particles ∼400−500 nm in size. More recently, Kuo et al.[26] synthe-

* To whom correspondence should be addressed. E-mail: frstella@mit.edu.
† MIT.
‡ Harvard University.

(1) Cui, Y.; Bjork, M. T.; Liddle, J. A.; Sonnichsen, C.; Boussert, B.; Alivisatos, A. P. *Nano Lett.* **2004**, *4*, 1093−1098.
(2) Dionne, J. A.; Sweatlock, L. A.; Atwater, H. A.; Polman, A. *Phys. Rev. B* **2005**, *72*, 075405.
(3) Maier, S. A.; Atwater, H. A. *J. Appl. Phys.* **2005**, *98*, 011101.
(4) Shubin, V. A.; Kim, W.; Safonov, V. P.; Sarychev, A. K.; Armstrong, R. L.; Shalaev, V. M. *J. Lightwave Technol.* **1999**, *17*, 2183−2190.
(5) Cao, Y. W. C.; Jin, R. C.; Mirkin, C. A. *Science* **2002**, *297*, 1536−1540.
(6) Lin, A. W. H.; Lewinski, N. A.; West, J. L.; Halas, N. J.; Drezek, R. A. *J. Biomed. Opt.* **2005**, *10*, 064035.
(7) Loo, C.; Lowery, A.; Halas, N.; West, J.; Drezek, R. *Nano Lett.* **2005**, *5*, 709−711.
(8) O'Neal, D. P.; Hirsch, L. R.; Halas, N. J.; Payne, J. D.; West, J. L. *Cancer Lett.* **2004**, *209*, 171−176.
(9) Narayanan, R.; El-Sayed, M. A. *J. Phys. Chem. B* **2005**, *109*, 12663−12676.
(10) Cui, Y.; Banin, U.; Bjork, M. T.; Alivisatos, A. P. *Nano Lett.* **2005**, *5*, 1519−1523.
(11) Millstone, J. E.; Park, S.; Shuford, K. L.; Qin, L. D.; Schatz, G. C.; Mirkin, C. A. *J. Am. Chem. Soc.* **2005**, *127*, 5312−5313.
(12) Murphy, C. J.; San, T. K.; Gole, A. M.; Orendorff, C. J.; Gao, J. X.; Gou, L.; Hunyadi, S. E.; Li, T. *J. Phys. Chem. B* **2005**, *109*, 13857−13870.
(13) Krahne, R.; Chilla, G.; Schueller, C.; Carbone, L.; Kudera, S.; Mannarini, G.; Manna, L.; Heitmann, D.; Cingolani, R. *Nano Lett.* **2006**, *6*, 478−482.
(14) Hao, E.; Schatz, G. C.; Hupp, J. T. *J. Fluoresc.* **2004**, *14*, 331−341.
(15) Jana, N. R.; Gearheart, L.; Murphy, C. J. *J. Phys. Chem. B* **2001**, *105*, 4065−4067.
(16) Chen, S. H.; Wang, Z. L.; Ballato, J.; Foulger, S. H.; Carroll, D. L. *J. Am. Chem. Soc.* **2003**, *125*, 16186−16187.
(17) Sau, T. K.; Murphy, C. J. *J. Am. Chem. Soc.* **2004**, *126*, 8648−8649.
(18) Sanedrin, R. G.; Georganopoulou, D. G.; Park, S.; Mirkin, C. A. *Adv. Mater.* **2005**, *17*, 1027−1031.
(19) Jin, R. C.; Cao, Y. W.; Mirkin, C. A.; Kelly, K. L.; Schatz, G. C.; Zheng, J. G. *Science* **2001**, *294*, 1901−1903.
(20) Kanaras, A. G.; Sonnichsen, C.; Liu, H. T.; Alivisatos, A. P. *Nano Lett.* **2005**, *5*, 2164−2167.
(21) Liu, H. T.; Alivisatos, A. P. *Nano Lett.* **2004**, *4*, 2397−2401.
(22) Manna, L.; Scher, E. C.; Alivisatos, A. P. *J. Am. Chem. Soc.* **2000**, *122*, 12700−12706.
(23) Manna, L.; Scher, E. C.; Alivisatos, A. P. *J. Cluster Sci.* **2002**, *13*, 521−532.
(24) Milliron, D. J.; Hughes, S. M.; Cui, Y.; Manna, L.; Li, J. B.; Wang, L. W.; Alivisatos, A. P. *Nature* **2004**, *430*, 190−195.
(25) Hao, E.; Bailey, R. C.; Schatz, G. C.; Hupp, J. T.; Li, S. Y. *Nano Lett.* **2004**, *4*, 327−330.
(26) Kuo, C.-H.; Huang, M. H. *Langmuir* **2005**, *21*, 2012−2016.

10.1021/cm060681i CCC: $33.50
Published on Web 06/17/2006

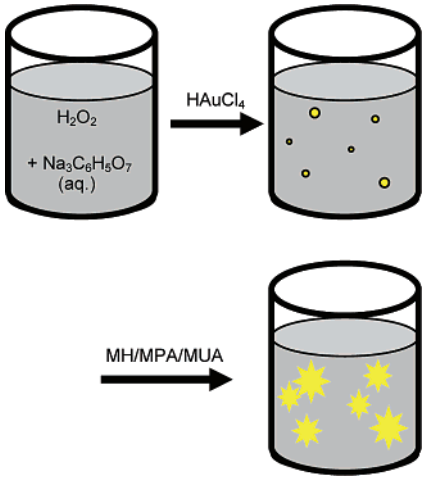

Figure 1. Schematic drawing of the main steps involved in the synthesis of the nano-urchins.

sized small (~40 nm in size) multi-branched (>4) gold nanoparticles, using a multi-step seeded growth approach with sodium dodecyl sulfate (SDS) as the surfactant. All of these methods result in particles only weakly stabilized by ligands electrostatically attracted to the metal cores; thus, all of these particles would coalesce irreversibly upon drying. The synthesis method reported in our paper results in small (~40 nm) multi-branched (>4) gold nanoparticles that differ from those reported in the literature mainly because of their thiolated capping molecules, which provide stability also in the dried state. The size of the nanoparticles, ~40 nm in diameter, ensures a strong plasmon response,[27] while the thiolated ligand shell improves the particles' solubility and stability as well as enhancing their versatility[28] as building blocks for composite nanostructures.

Materials and Methods

All chemicals were purchased from Sigma Aldrich and used as received. Ultrapure Millipore water (18 MΩ) was used as a solvent. Nanoparticle images were taken using either a JEOL 2000 FX or a JEOL 200 CX transmission electron microscope (TEM) at 200 kV accelerating voltage. UV−vis absorption spectroscopy was done using an Agilent 8453 diode array absorption spectrometer.

Nanoparticle Synthesis. In a typical synthesis, 6.5 μL of a 35 vol % water solution of H_2O_2 was added to 10 mL of a 6.8×10^{-3} M solution of sodium citrate. A total of 25 μL of a 0.05 M $HAuCl_4$ water solution was added dropwise over a period of 120 s. Stirring was stopped 10 s after the addition was completed. During the addition, the color of the solution changed from transparent to purple. Within less than a minute (i.e., ~150 s after the complete addition of $HAuCl_4$), 1.05 mL of a 7.5 mM aqueous solution of a thiolated molecule was added dropwise while stirring. The ligand molecules used were 11-mercapto-1-hexanol (MH), 3-mercapto-propanoic acid (MPA), and 11- mercaptoundecanoic acid (MUA). When mixtures of the ligands were used, the total concentration was kept at 7.5 mM. In the case of MUA, it was necessary to add NaOH (~1:5 molar ratio) to make the thiol molecule soluble in water. Figure 1 illustrates the main steps involved in the synthesis.

(27) El-Sayed, M. A. *Acc. Chem. Res.* **2001**, *34*, 257−264.
(28) Wanunu, M.; Popovitz-Biro, R.; Cohen, H.; Vaskevich, A.; Rubinstein, I. *J. Am. Chem. Soc.* **2005**, *127*, 9207−9215.

Results and Discussion

As illustrated in Figure 1, the first step of the reaction presented here consists of reducing gold ions using H_2O_2. The solution changes color during the addition of $HAuCl_4$-(aq) to the reaction vessel. The rate of addition seems to strongly influence the solution color and thus probably the shape of the particles obtained. We have isolated the intermediate product of our reaction and found that it mostly consists of spheroidal particles (>90%) with the presence of a few tripods. Upon addition of thiolated molecules, the color of the purple solution becomes more bluish. This happens with MPA, MUA, MH, and with binary mixtures of any of these thiols. The nanoparticles remain stable in solution and can be stored in a refrigerator for about a week, or alternatively, the solvent can be removed and the nanoparticles can be stored in the solid state for at least several weeks and redissolved whenever needed. Particles made using just MH as a ligand were an exception because they showed signs of color loss in a matter of minutes after the synthesis was completed and complete precipitation of the nanoparticles within hours, after which the nanoparticles were insoluble.

Samples from the solutions were drop cast onto carbon coated TEM grids. Representative images are shown in Figure 2. A large fraction of particles with a number of marked protuberances is evident. More than 90% of the particles have four or more branches, and the majority of the particles (~70%) have five or more branches. Most particles have a studded quasi-spherical morphology resembling sea urchins. The size and morphology of the nanoparticles depend strongly on the rate of the addition of $HAuCl_4$(aq). We have been able to reproducibly synthesize nano-urchins that have a mean diameter of ~40 nm with a standard deviation of ~10 nm (see Figure 2; note that the diameter of the particles is defined as its biggest dimension).

UV−vis extinction spectra of the synthesized nanoparticle solutions were measured. A typical spectrum is shown in Figure 3. The absorbance exhibits a strong and relatively narrow plasmon resonance peak around ~585 nm. The strong plasmon is to be expected from the sharp topological features of the nano-urchins. The relative narrow full width at half-maximum (fwhm = 138 nm with a standard deviation of 7 nm based on a comparison across the various samples synthesized in this paper) of the peak may seem counter to intuition, given the broad distribution of shapes and sizes of the nanoparticles in our samples (Figure 2). However, we reason that the lack in broadening in our extinction spectra is in agreement with the simulations done by Hao et al.[25] on metal tripods. They showed that the dipole excitation from the tips of the branches of the tripod provides the dominant contribution to the plasmon resonance in the extinction spectrum, and therefore, any heterogeneity in the shape of the branches, and in their number, should have only a negligible effect on the spectrum. As mentioned before, the nanoparticle solution may be dried, for example, to store the particles for longer periods of time. We find that, with the exception of pure MH coated nano-urchins, the rest of the particles can be dissolved back in water and remain stable in solution. However, the optical properties of the redissolved

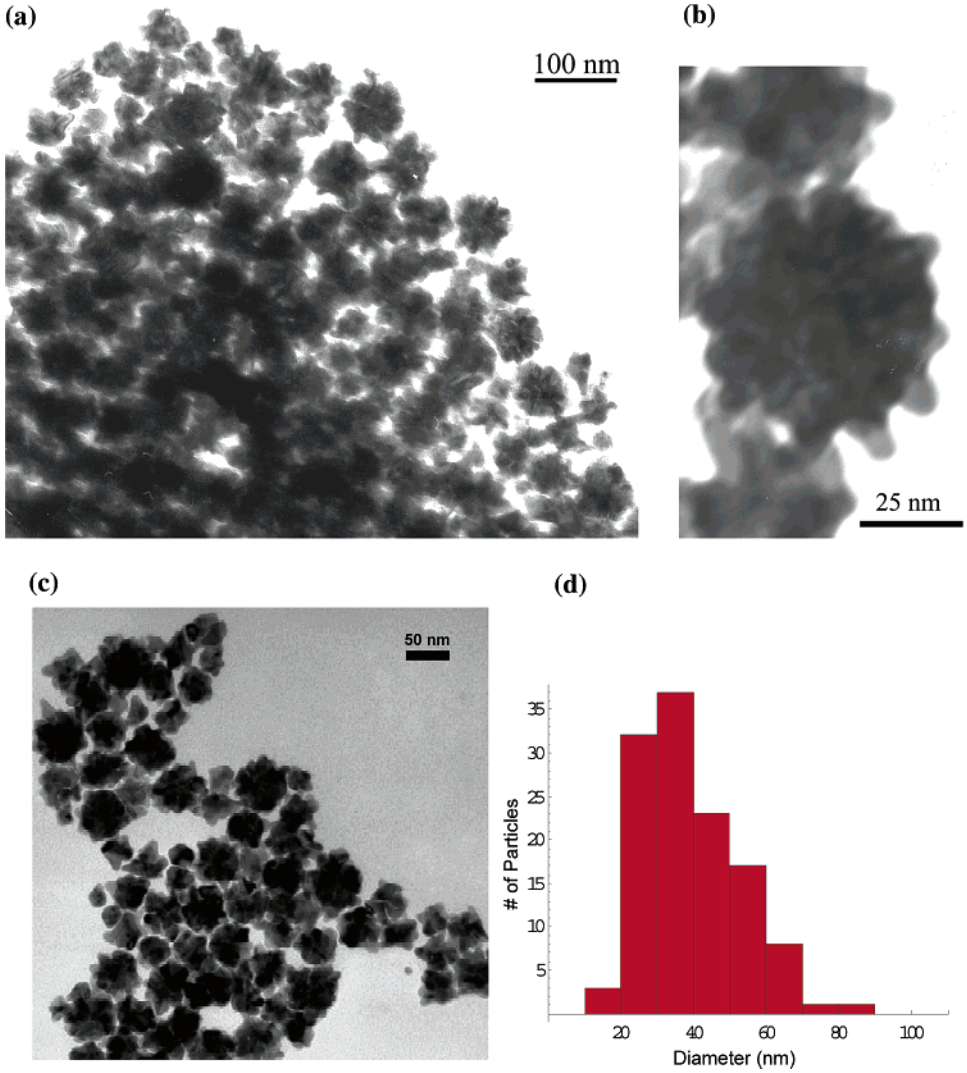

Figure 2. Representative TEM images of nanoparticles obtained using the synthesis approach presented here. (a and b) Images of a sample synthesized with a mixture of MH and MPA in a 1:1 molar ratio. (c) Image of a sample synthesized with a mixture of MH and MUA (1:1). (d) Histogram showing the distribution of nanoparticle sizes observed in sample shown in panel c.

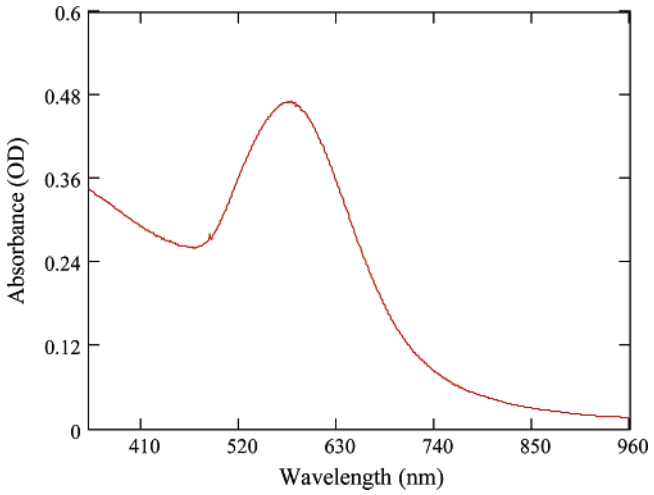

Figure 3. Plot of the extinction spectrum of nano-urchins in water. This spectrum is of nano-urchins synthesized with a mixture of MUA and MH in a 1:1 molar ratio.

particles suggest that they dissolve in an aggregate form. Figure 4 shows a comparison between spectra of the nano-urchins taken right after they were synthesized and after being dried and dissolved again. The red-shift and the broadening of the extinction peak strongly suggest a form of aggregation. It should be noted that the new extinction spectrum does not evolve if the particles are dried and redissolved again; it remains fairly constant. Also, upon sonication, the peak narrows and blue-shifts toward an intermediate state between the initial and the aggregate state, presumably due to a reduction in the size of the aggregates. TEM samples drop cast from these solutions (after sonication) indicated that the particles maintained their urchin-like morphology, with no observable changes in their size distribution or shape (Figure 4).

Finite difference time domain (FDTD) simulations are a versatile numerical method for solving electromagnetic problems of arbitrary shapes and geometries that are otherwise difficult to solve for analytically.[29,30] FDTD simulations were used to investigate the near-field enhancements in the vicinity of a nanoparticle with horns whose dimensions are similar to the ones observed in the nano-urchins synthesized in this work. The simulation was run

(29) Yee, K. S. *IEEE Trans. Antennas Propag.* **1966**, *14*, 302.
(30) Taflove, A.; Brodwin, M. E. *IEEE Trans. Microwave Theory Tech.* **1975**, *23*, 623−630.

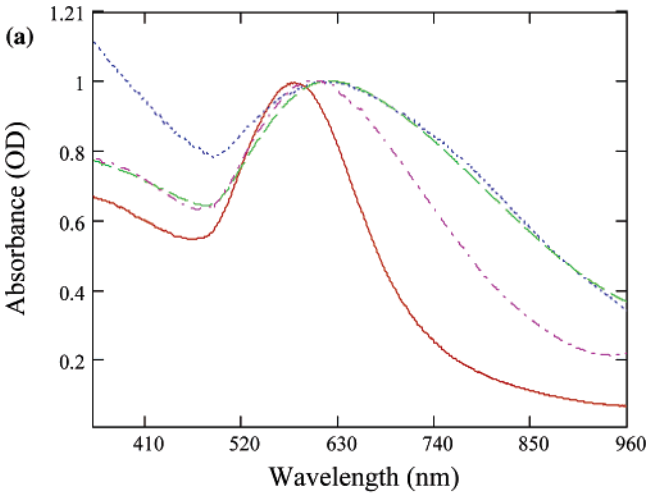

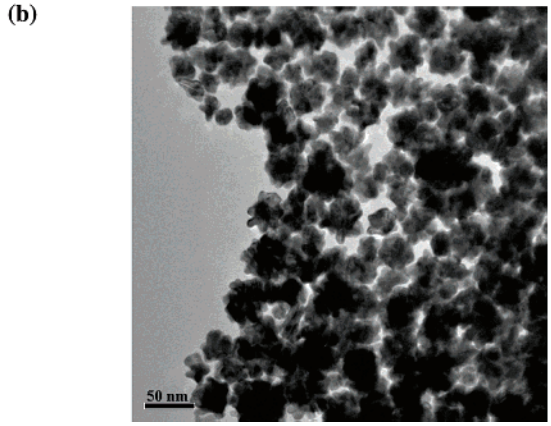

Figure 4. (a) Plot of the extinction spectra of MUA capped nano-urchins in water. The spectrum on the first day (red continuous line) was taken right after synthesis. After the measurement, the sample was dried and kept in the fridge for 6 days. It was then redissolved in water to allow for optical characterization and then dried again. This operation was repeated at the ninth (blue dotted line) and tenth day (green dashed line). The latter solution was sonicated for 30 min, leading to the purple dash dotted spectrum. All spectra had their peak maximum normalized to unity. (b) TEM image taken from the solution obtained after 10 days of storing after sonication.

on a tetrapod with its horns (i.e., branches) sticking out in a manner similar to carbon sp^3 bonding orbitals. The horns were modeled as pyramids with an equilateral triangular base (side length = 12.4 nm) 15 nm long and with an apex truncated parallel to the base (side length = 5.7 nm) (Figure 5a). The overall tetrapod dimension was 37 nm using the convention defined previously. The base of one of the horns was set to be parallel to the *xy* plane, centered at the origin ($x = 0$, $y = 0$, $z = 0$).

The simulations were done at 13 wavelengths, for which an experimental dielectric constant for bulk gold was found,[31] covering the 300−1200 nm range. The incident electromagnetic field was chosen to be a continuous monochromatic plane wave polarized in the *z* direction with a wave vector in the negative *x* direction. The simulations were run until a steady state was reached. The computational space was divided into cubic cells with 3 Å sides. This was more than sufficient to accurately approximate the given geometry. All simulations were run on a commercial FDTD package (RemCom XFDTD version 6.1). The default Liao Absorbing boundary condition was used to bind the computational space, so that scattered or emitted radiation from tetrapods was absorbed by the boundary with minimum reflection.[32]

Figure 5b shows the maximum intensity (i.e., square of the field strength) enhancement of the electric field observed near the tip horns of the tetrapod as a function of the wavelength of the incident field. These quantities were taken at steady state, when all the scattered fields also varied sinosoidally in time. As can be seen, the resonance frequency occurs at around 700 nm. The enhancement in the local field intensity near the tips is ∼15 000 times the intensity of the incident field.

Figure 5c shows a contour plot of the calculated magnitude of electric field distribution, at the resonance frequency, around the tetrapod in a plane that goes through two of its tips. As expected, the field is largest near the tips. However, it may be noticed that most of the resonant excitation is localized around one of the two tips. This is because the tetrapod geometry is highly anisotropic, so the choice of which horn to excite depends strongly on the choice of the incident electromagnetic field and its polarization. The hot spots of large field enhancements near the tips are ideal locations for the placement of molecules for the purpose of SERS experiments.[33−36] This task is made easier in the case of nano-urchins such as the ones in Figure 2 since these particles have many horns, and therefore, the hot spots are expected to be abundant.

The simulated spectrum of the tetrapod has some similarities and differences when compared to the nano-urchins. Both have a single plasmon resonance peak, but the tetrapod's peak is red-shifted by ∼120 nm with respect to the peak observed in the extinction spectrum of the nano-urchins. This can be qualitatively explained within the framework of plasmon hybridization theory[37] based on the morphology of the nano-urchins, which is a hybrid between a sphere and a purely branched particle such as the tetrapod. Whereas gold nanospheres and tetrapods have their plasmon resonance at ∼540 and ∼700 nm, respectively, nano-urchins have their resonance somewhere between ∼585 nm.

Finally, the ∼15 000 times local field intensity enhancement predicted in the FDTD calculation is an enormous improvement over the enhancements observed near isolated spherical nanoparticles, which only show enhancements on the order of only several hundred times.[38] This is important for SERS experiments given that the Raman scattering cross-section is proportional to the fourth power of the local field.[36] However, some concerns might arise regarding the choice of bulk gold properties in the FDTD simulation since it is

(31) Johnson, P. B.; Christy, R. W. *Phys. Rev. B: Solid State* **1972**, *6*, 4370−4379.
(32) Liao, Z. P.; Wong, H. L.; Yang, B.; Yuan, Y. *Sci. Sin. Ser. A: (Engl. Ed.)* **1984**, *27*, 1063−1076.
(33) Otto, A. In *Light Scattering in Solids IV: Electronic Scattering, Spin Effects, SERS, and Morphic Effects*; Cardona, M., Güntherodt, G., Eds.; Springer-Verlag: Berlin, 1984.
(34) Moskovits, M. *Rev. Mod. Phys.* **1985**, *57*, 783−826.
(35) Zeman, E. J.; Schatz, G. C. *J. Phys. Chem.* **1987**, *91*, 634−643.
(36) Kall, M.; Xu, H. X.; Johansson, P. *J. Raman Spectrosc.* **2005**, *36*, 510−514.
(37) Prodan, E.; Radloff, C.; Halas, N. J.; Nordlander, P. *Science* **2003**, *302*, 419−422.
(38) Shalaev, V. M. In *Optical Properties of Nanostructured Random Media*; Shalaev, V. M., Ed.; Springer-Verlag: Berlin, 2002; p 99.

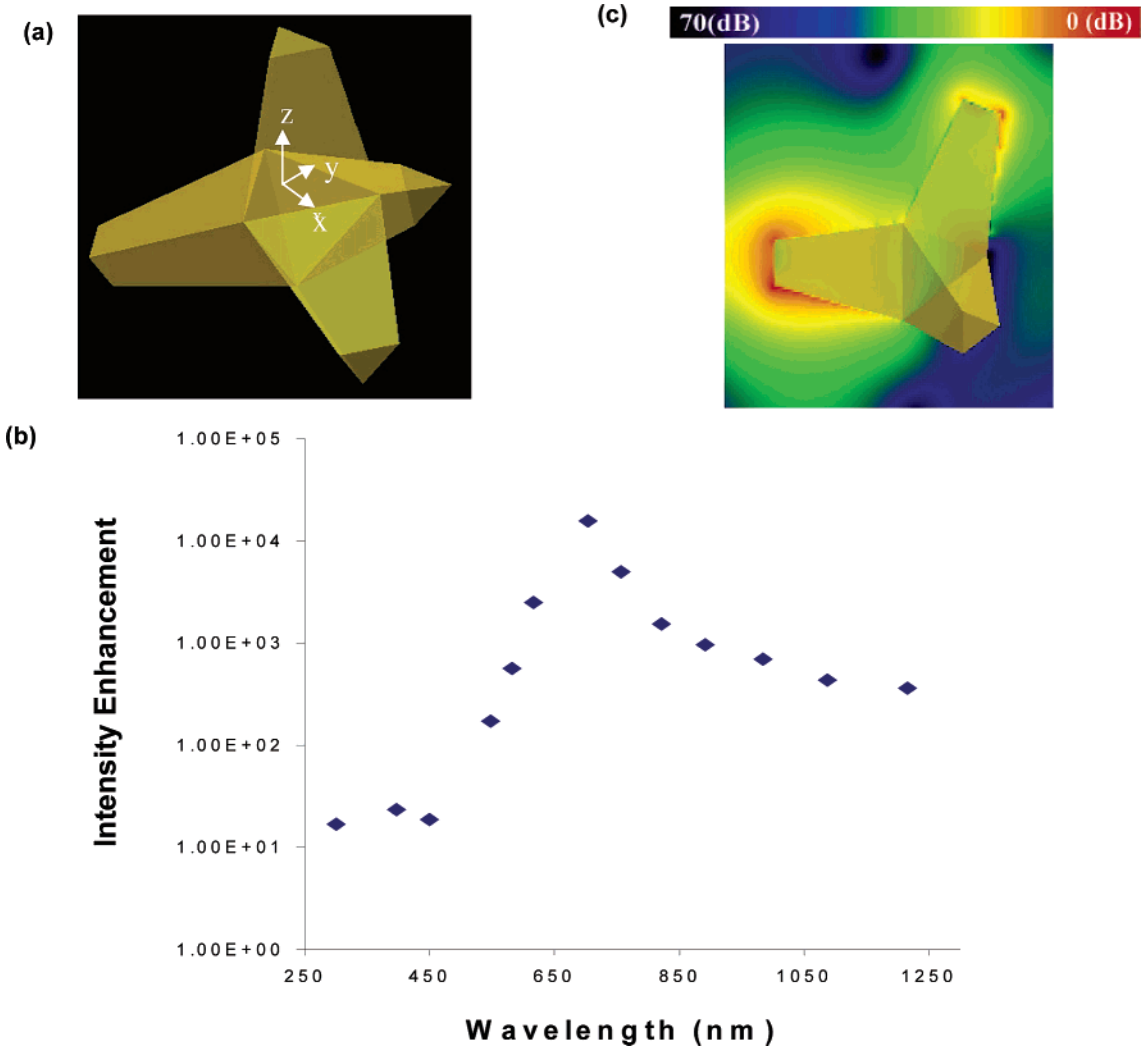

Figure 5. (a) Drawing of the tetrapod geometry used in the FDTD simulations and its dimensions. (b) Plot of the wavelength vs the maximum intensity enhancement as calculated by FDTD for the tetrapod pictured in panel a. Light is traveling with a wave vector in the negative *x* direction and is *z* polarized. (c) Contour plot of the calculated distribution of electric field strengths around the tetrapod in a plane that cuts through the tips of the upper horn and left most horn. The scale is in decibels (dB). The maximum (dB = 0) corresponds to an electric field magnitude of 125 V/m.

well-known that the dimensions of the nanoparticle can constrain the mean free path of the electrons.[39] The real part of the dielectric constant of the gold nanoparticles does not deviate significantly from its bulk value, but the imaginary part significantly increases for spherical nanoparticles less than 12 nm in diameter.[40] An increase in the imaginary part of the dielectric constant results in the dampening of the resonance enhancement. And so, to be conservative, we repeated the FDTD calculation at 704 nm using the imaginary part of the dielectric constant that was experimentally determined by others for a 9 nm diameter nanoparticle.[41] The calculation resulted in a local field enhancement of ~2950 times, which is still much larger than the enhancement observed in isolated spherical nanoparticles.[38]

Conclusion

In conclusion, here we have presented a method for the synthesis of gold multi-pods with more than four branches in high yield using MH, MUA, MPA, and binary mixtures of these thiols as capping agents. The particles are stable and water soluble, and they can be stored for days in the dried state and redissolved many times. After drying, the particles dissolve in a stable and reproducible aggregate form. FDTD calculations performed on a nanoparticle with four branches suggest that nano-urchins have large local electromagnetic field enhancements near the tips of their horns. The plasmon resonance peak of these particles is narrow and has a fwhm that is almost invariant with particle size and shape distribution, suggesting that the dipole of the plasmon is mostly concentrated at the tips of the multi-pods. These particles may find applications in SERS and in catalysis.

Acknowledgment. The financial support of the National Science Foundation (NIRT DMR-0303973), the National Health Institute (TPEN), and the Petroleum Research Fund is kindly acknowledged. F.S. is grateful to 3M and to DuPont for the young faculty awards. O.M.B. acknowledges the generous support of the Saudi Ministry of Higher Education and the Saudi Arabian Cultural Mission in the United States.

CM060681I

(39) Kreibig, U.; von Fragstein, C. *Z. Phys.* **1969**, *224*, 307−323.
(40) Doremus, R. I. *J. Chem. Phys.* **1964**, *40*, 2389.
(41) Scaffardi, L. B.; Pellegri, N.; de Sanctis, O.; Tocho, J. O. *Nanotechnology* **2005**, *16*, 158−163.